Journal of Environment and Sustainable Mining Vol.1 No.4 (2025) 25-50

Journal of Environment and Sustainable Mining

Statistical Analysis of Geochemical Data in the Shadan Mineral District Using a Compositional Data Approach

Hassan Hosseinzadeh [1*], **Gholamreza Nowrouzi**[1]

[1] Department of Mining Engineering, Engineering Faculty, Birjand University, Birjand, Iran.

ARTICLE INFO

Article type:
Research Article

Article history:
Received: 2025-10-10
Received in revised form: 2025-11-29
Accepted: 2025-12-22
Available online: 2025-12-29

Keywords:
Shadan,
Compositional,
Statistics,
Robust factor analysis,
Geochemical rock samples

ABSTRACT

This study aims to evaluate the mineralization potential of the Shadan area based on the geochemical analysis of 300 rock samples. Due to the compositional nature of geochemical data, the Centered Log-Ratio (CLR) transformation was applied to address the closure problem and enable meaningful statistical interpretation. Subsequently, fractal modeling using the concentration-area–area (C–A) relationship was employed to delineate geochemical anomalies where elemental concentrations increase significantly. In these anomalous zones, copper (Cu) concentrations reached up to 0.47 wt%, gold (Au) up to 2.5 g/t, and molybdenum (Mo) up to 56 ppm. To better understand the underlying geochemical structure, robust factor analysis was conducted. This method minimizes the influence of outliers and provides more reliable factor patterns in complex geological settings. The analysis identified a dominant factor with strong negative loadings for Cu, Au, and Mo, indicating a clear geochemical association and a possible shared origin through mineralization processes. Spatial interpretation revealed that these anomalies are closely associated with intrusive bodies of quartz diorite to granodiorite, lithological units commonly linked to porphyry-type systems. Additional element associations were observed between Ni–Cr and Pb–Zn, suggesting the influence of deep mafic–ultramafic magmatic sources and zoned hydrothermal systems, respectively. These findings confirm the significant role of magmatic and hydrothermal processes in the enrichment of ore elements in the Shadan region. Overall, the results indicate that the Shadan area hosts a well-developed porphyry system and represents a promising target for further mineral exploration, particularly for Cu, Au, and Mo.

Cite this article: Hosseinzadeh, H. and Nowrouzi, G. (2025). Statistical Analysis of Geochemical Data in the Shadan Mineral District Using a Compositional Data Approach. *Journal of Environment and Sustainable Mining*, 1(4), 25-50. https//doi.org/10.22111/jesm.2025.52412.1031

Publisher: University of Sistan and Baluchestan.
DOI: https//doi.org/10.22111/jesm.2025.52412.1031

* Corresponding author: **Hassan Hosseinzadeh**
E-mail address: hosseinzadeh.hassan70@gmail.com

1 .Introduction

Exploratory geochemistry has emerged as a key tool in the search for low-grade mineral deposits, particularly those that are challenging to detect through traditional means, such as certain porphyry deposits [1, 2]. Geochemical methods can be applied at various stages of mineral resource exploration and are based on identifying areas where the concentration of specific elements exceeds normal levels. In other words, geochemical exploration aims to detect geochemical anomalies that may indicate the presence of mineralization. It is important to emphasize that geochemistry does not pinpoint the exact location of a deposit. Instead, it identifies indirect indicators that suggest the presence of mineral deposits or favorable geological conditions for their formation. These geochemical signals are typically detectable at the surface only when the deposit is relatively large and not deeply buried. In such cases, surface geochemical markers may be observed, particularly if they contrast significantly with the background geochemical properties of the surrounding rocks. When this contrast exists, a geochemical anomaly can be defined [3].

Geochemical methods are classified based on their operational principles or the types of materials analyzed. One common approach is the geochemical analysis of rock samples. This method is particularly effective for discovering concealed mineralization, especially in mountainous terrains. Rock samples are usually collected from surface outcrops of geological units [4]. Geochemical investigations involve several stages, including survey design, sampling, sample preparation, laboratory analysis, pre-processing, and data processing. These steps ultimately lead to the creation of elemental distribution maps, anomaly detection, and interpretation. Due to the compositional nature of geochemical data, this study applied compositional data analysis techniques during both pre-processing and interpretation phases.

Because geochemical data are compositional and closed (i.e., their values represent relative proportions that sum to a constant), changes in one element inherently affect all others. As a result, traditional statistical methods—which assume variable independence—are not suitable and may yield misleading results [5, 6]. To address this, compositional statistical methods were employed in this study to analyze geochemical data from the Shadan area, as discussed in the following sections.

2. Research Background

To better understand the differences and advantages of using compositional statistical methods compared to simple statistical methods in geochemical data analysis, it is essential to examine the various aspects of both approaches. Geochemical data are often of a closed and compositional nature, meaning that these data are not only inherently dependent but also constrained to a constant sum (such as 100%). These characteristics pose significant challenges when using traditional, simple statistical methods. In geochemical data analysis, there are substantial differences between the application of simple statistical methods and compositional statistical methods, which impact the accuracy and results of the analysis. Typically, geochemical data are closed and compositional, meaning that their values are interdependent and constrained to a fixed sum [6]. These features make traditional statistical methods, which assume independence among variables, prone to inaccuracies and misleading interpretations.

In simple statistical methods, it is assumed that the variables are independent of one another, and each element has a separate effect [7]. For example, correlation and regression analyses in these approaches usually disregard these internal dependencies, leading to errors in interpreting relationships between geochemical elements [5, 8]. On the other hand, compositional statistical methods, such as log-ratio transformations (CLR or ILR), specifically designed for closed data, account for these internal dependencies by transforming closed data into a non-closed form, enabling more accurate analysis [6, 9]. Additionally, in correlation analysis, compositional methods offer greater precision. For instance, a study by Martinez (2012) demonstrated that using the CLR method for correlation analysis of geochemical data provided much more reliable results compared to traditional methods that ignore internal dependencies. In managing censored and missing data, compositional methods such as ILR-EM also outperform simple methods [10]. These methods are particularly effective in replacing censored data and considering the compositional nature of the data, whereas simple methods often remove or inadequately replace such data, reducing analytical accuracy [11]. In multivariate analyses, compositional statistical methods like CoDa-

PCA (Principal Component Analysis for Compositional Data) have been shown to provide more accurate results compared to traditional methods. For example, Filzmoser (2009) demonstrated in a study that CoDa-PCA could correctly identify more complex patterns among geochemical elements, whereas traditional methods often lead to incorrect interpretations of these relationships [8].

To clarify these points further, let us consider some significant and related studies in this field. Reimann (2002), in his research, emphasized the importance of analyzing compositional data in geochemical studies, showing that the use of simple statistical methods, such as linear correlations without accounting for the closed nature of data, could lead to incorrect interpretations of relationships between elements. This study specifically highlighted that the use of CLR and ILR transformations could improve the accuracy of analyses [12]. In later years, Filzmoser (2009) explored the challenges of compositional data in multivariate analysis. They demonstrated that traditional Principal Component Analysis (PCA) methods are unsuitable for compositional data, and the use of CoDa-PCA, specifically designed for closed data, can lead to more accurate results in identifying hidden patterns in geochemical data [8]. Martin et al. (2012), by introducing robust methods in the analysis of compositional data, such as "Compositional Robust Factor Analysis," demonstrated that these methods are highly effective in dealing with unstable and outlier data, helping to identify more accurate and deeper relationships between geochemical elements. This study provided real-world geochemical data examples, showing that using robust methods significantly improves the precision of multivariate analyses [13]. In recent years, Pawlowski (2015) addressed the importance of applying compositional methods in geochemical studies, showing that using compositional approaches can provide more accurate information about element distribution patterns in mineral environments. This study comprehensively reviewed the various advantages and challenges of compositional methods and is regarded as one of the key resources in this field [14]. Hikaru et al. (2017), using compositional analysis methods in geochemical data, investigated mineral potentials and showed that employing robust principal component analysis for closed data significantly improves the precision of identifying geochemical anomalies. This research is particularly important for identifying promising regions for mineral exploration [15]. In a more recent study, Lin et al. (2020) used compositional methods to analyze geochemical data from a mineral region in China. They demonstrated that CLR and ILR methods for analyzing geochemical data could reveal complex patterns and hidden relationships between elements that are not observable using simple statistical methods. This study particularly emphasized the importance of using compositional methods in mineral exploration studies [16].

Collectively, these studies, along with other research conducted in this field [3, 17-20], demonstrate that compositional statistical methods offer significant advantages over traditional, simple methods in geochemical data analysis, contributing to more accurate identification of mineral potentials and the complex relationships between geochemical elements.

3. Geology and Geochemical Data of the Study Area

The Shadan area is located 65 kilometers south of Birjand city, near the village of Sheikh Abad, in South Khorasan Province, Iran. This region lies within the 1:100,000 Sar Chah Shur geological map. The volcanic facies and their alteration processes in various zones, along with proximity to the Lut Desert, are major factors influencing the morphological features of this region. In the northern and western parts, volcanic morphology is prominent, characterized by steep elevations and numerous rocky cliffs. The central and southern parts of the area are composed of foothills and low-lying hills. To the south and west, the region transitions into the Lut Desert, with alluvial fans formed by eroded material from the highlands, acting as a connection between this area and the desert plains.

From a structural geology perspective, the study area is located on the eastern margin of the Lut Block. More than 17 intrusive bodies, ranging in composition from acidic to intermediate, including diorite to syenite, have been identified in this region. The 1:1,000 geological map of the area is presented in Fig. 1. The hydrothermal alteration zones associated with the intrusive bodies include argillic, propylitic, advanced argillic, silicic, quartz-sericite-pyrite, gossan, and hydrothermal breccia zones, which often overlap. This overlap, coupled with intense weathering, creates challenges in distinguishing the alteration zones.

Mineralization in the area is primarily sulfide-based, consisting of pyrite and, to a lesser extent, chalcopyrite, with iron oxides present as disseminated grains and quartz-iron oxide stockwork veins.

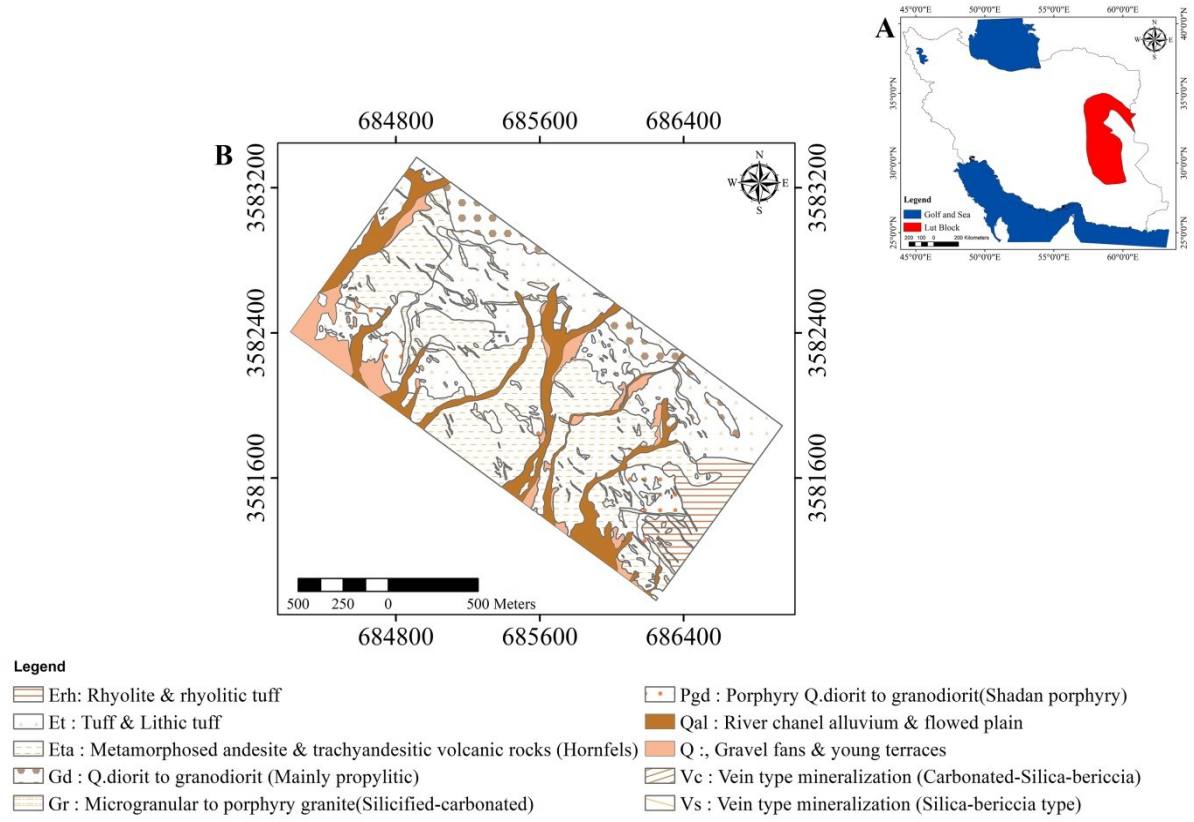

Fig. 1. A: Location of the Lut Block in Eastern Iran, B: 1:1000 Scale Geological Map of the Shadan Area.

Based on the geological map, this area comprises porphyritic andesitic rocks, Eocene volcanic rocks, tuffs, lavas, pyroxene andesites, and intrusive microdiorites, with occasional occurrences of monzonite and quartz monzonite. While microdiorite is more widespread than the andesitic porphyry bodies, mineralization is observed in an altered monzonite intrusive phase in the northeastern section. Additionally, tourmaline, often associated with carbonate, is more prevalent in the eastern part of the region, which can be referred to as the listvenite zone. In the central part of the region, signs of potassic alteration in an andesitic-microdioritic mass are observed, with gray quartz veins containing malachite and limonite. This area is covered by moderate argillaceous alteration, which has likely contributed to an increase in sulfide-quartz veins. In the eastern part, malachite and sheet quartz veins are visible, along with explosive breccia, actinolite, and coarse-grained quartz. To the north and east of the area, propylitic alteration (chlorite, epidote, pyrite) affects the andesites, volcanoclastic rocks, and tuffs. The region contains numerous faults, which can be categorized into two main groups: those trending northwest to southeast, which are followed by dikes with the same trend, and a second group trending northeast to southwest. North-south trending faults with shorter lengths are also present, though their impact is less pronounced. In the northern and eastern parts of the region, tectonic activity is more significant. There is a close relationship between the presence of faults, lineaments, alteration, and mineralization. The study area, in terms of Iran's geological divisions, is part of the Lut Block, the Central Iranian microcontinent, and the eastern Iran ophiolite-tectonic belt, sharing features of both regions. The Lut Block, approximately 900 kilometers in length, is bounded

by the Nayband Fault to the west and the Nehbandan Fault to the east. It is bordered to the north by the Doruneh Fault and to the south by the Jazmurian Depression.

In the Shadan area, a total of 300 rock samples, primarily from intermediate to acidic rocks and associated with alteration zones, have been systematically collected. The sampling was conducted based on a designed grid network. After initial preparation stages, the samples were subjected to chemical analysis for 46 elements using ICP-OES, and Au analysis was performed using the Fire Assay method. The geographical distribution of the samples collected from the Shadan area is presented in Fig. 2.

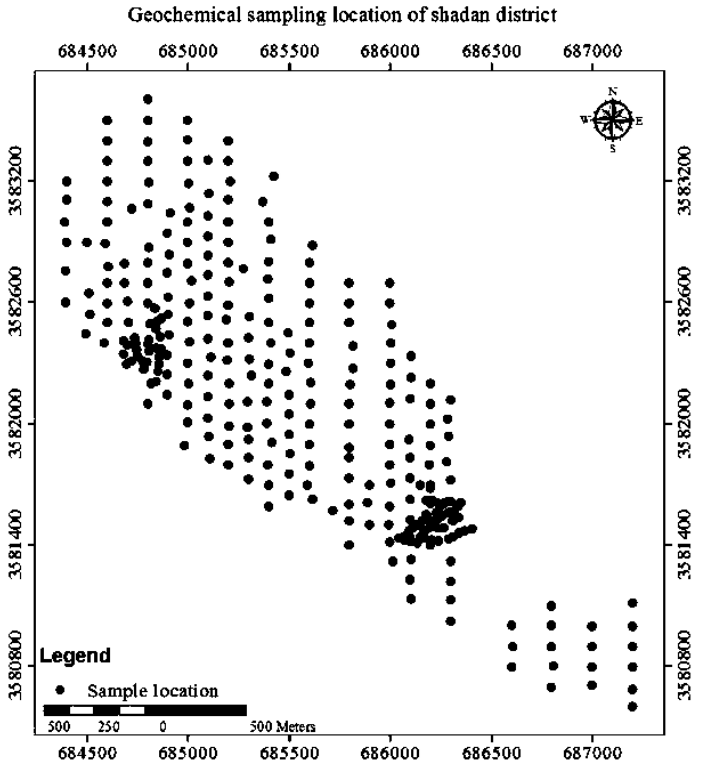

Fig. 2. Geochemical Sample Locations in the Shadan Area.

4. Compositional Data

Compositional data refers to data containing relative information, meaning they represent parts of a whole. In most cases, these data are referred to as closed data, as they have a constant sum. A classic example of a closed array or closed numerical system is a dataset where the variables are not independent and are expressed as percentages or parts per million (ppm) [5, 8]. Geochemical analyses are typical examples of composite data. For instance, in a sample taken from an igneous rock, if the SiO2 content accounts for 69% of the rock's composition, the remaining components, such as MgO, will make up the other 31%. This implies that an increase in one component necessarily leads to a decrease in the other components. Previously, datasets with a constant sum were referred to as composite data, but currently, this term has a broader definition and includes datasets that do not necessarily have a constant sum [21].

Composite data has specific properties that prevent the use of standard statistical methods for its analysis. Euclidean space is not suitable for composite data, as the constant sum constraint implies a unique geometry known as Aitchison geometry in the simplified space [5, 8]. To apply standard statistical methods, appropriate transformations must be applied to the data. One of these transformations is the family of logarithmic transformations, first introduced by Aitchison (1982) [6]. Statistical methods are applied to the transformed data, and the results are back-transformed to the original space.

4.1. Transformations for Composite Data

Several transformations have been proposed for the statistical analysis of composite data. The geometry of composite data is referred to as Aitchison geometry. Fortunately, there is an appropriate method for transforming composite data from a simplified sample space to Euclidean space, known as log-ratio transformations.

The sample space of closed data for a D-part composition $X = (x_1, \dots, x_D)$is defined as follows:

$$S^D = \left\{ X = (x_1, \dots, x_D) \middle| x_i > 0, i = 1,2, \dots, D; \sum_{i=1}^{D} x_i = k \right\} \quad (1)$$

In the above relation, the constant k varies depending on the measurement unit of the dataset, such as 100 for percentage data or $10^{\wedge 6}$ for ppm data.

Three types of logarithmic transformations are presented for unlocking composite data:

1. Additive Log-Ratio Transformation (alr) introduced by [6] is represented as:

$$alr(x) = y_i = ln \frac{x_i}{x_D} \qquad (i = 1,2, \dots, D-1) \quad (2)$$

Thus, one component with index j (chosen arbitrarily) is selected for the denominator of the ratios.

2. Centered Log-Ratio Transformation (clr), also introduced by [6], leads to a multivariate observation and is defined as:

$$clr(x) = y_i = ln \frac{x_1}{\sqrt{\prod_{i=1}^{D} x_i}} \qquad (i = 1,2, \dots, D-1) \quad (3)$$

By definition, $y_1+\cdots+y_D=0$, and the denominator of each ratio is the geometric mean of the observations.

3. Isometric Log-Ratio Transformation (ilr) introduced by [9] produces a multivariate observation in a (D-1)-dimensional space, making the interpretation of the data difficult. It is calculated according to the following equation:

$$ilr(x) = y_i = \sqrt{\frac{D-i}{D-i+1}}\, ln \frac{x_i}{\sqrt[D-i]{\prod_{j=i+1}^{D} x_j}} \qquad (i = 1,2, \dots, D-1) \quad (4)$$

Filzmoser (2009) argues that, apart from these three relative log-ratio transformations, no other transformations are suitable for unlocking composite variables for statistical analysis.

Some key features of these transformations, as discussed in various studies, are summarized below:

- All variables analyzed through these transformations must have consistent units.
- In the alr transformation, the variables are divided by an expert-chosen variable, making the results highly dependent on the expert's choice [6]. To address this issue, the clr transformation is defined, dividing each sample by its geometric mean.
- The alr and ilr transformations reduce the dimensionality of variables from S^D in Aitchison geometry to R^{D-1} in Euclidean geometry. However, the clr transformation provides a one-to-one mapping from Aitchison space to Euclidean space (R^D), making the data more interpretable, particularly in the univariate case [5, 7, 8].
- No changes occur in the statistical parameters of the original and transformed data, such as skewness or kurtosis, and the statistical distribution of univariate data remains unchanged. Only the ilr and simple logarithmic transformations may bring the data distribution closer to normality.
- In the case of ilr transformation, it is unclear how to handle the remaining components in univariate analyses and which ratio corresponds to which variable. To address this, Filzmoser (2009) suggests the following relation for the ilr transformation of any desired variable:

$$Z_1 = \sqrt{\frac{D-1}{D}}\ ln\frac{x_1}{\sqrt[D-1]{\prod_{j=2}^{D} x_j}} \quad (5)$$

- Since raw data are used in these transformations, outliers in the dataset can introduce errors in subsequent analysis stages. To mitigate the effect of outliers, robust statistical methods are recommended, whose effectiveness has been demonstrated in numerous studies [22].

- Robust methods are not compatible with data transformed by clr [23]. Thus, the ilr transformation should be applied first, and then the resulting weights and scores should be back-transformed into clr space to interpret the variables [5, 8].

- One of the advantages of using logarithmic transformations is the lack of need for data normalization after applying the transformations.

4.2. Geochemical Data Preprocessing

Preprocessing is the most crucial step in geochemical studies. Traditional univariate statistical tools, complex spatial statistical techniques, and multivariate statistical methods are employed for data description and analysis. Estimating censored data, replacing missing values, performing basic statistical analysis, identifying and correcting outliers, and applying necessary logarithmic transformations to ensure accurate data analysis are essential steps. Missing data is an inevitable issue in geochemical datasets. One common reason for missing data is values below the detection limit of the measurement device (censored data). Missing values in a dataset pose limitations on calculations and the use of statistical methods such as robust factor analysis, which require a complete dataset. A common solution to this problem is to remove samples with missing values, known as complete case analysis (CCA). However, using this method leads to biased results and loss of information. Instead of removing missing samples, missing cells in the dataset can be imputed with a suitable value. It is widely noted in literature that missing data imputation methods should not introduce significant changes to the overall data structure. Various methods for missing data imputation have been proposed, including a method by Heron et al., which has recently been applied to geochemical data analysis, as well as simple multiplicative replacement, log-normal multiplicative replacement, the EM algorithm, and DA in the log-transformed space. A study by Hosseini et al. (2015) shows that the ilr-EM algorithm is superior to other methods [24]. In this research, the ilr-EM method was used for imputing censored data. The elements with censored data and their quantities are listed in Table 1.

Table 1. Elements containing sensor data.

Element	Sensor data	PPM	Element	Sensor data	PPM	Element	Sensor data	PPM
Ag	204	68	Ni	2	0.66	La	1	0.33
As	34	11.33	Pb	2	0.66	Th	204	68
B	78	26	Rb	182	60.6	Li	2	0.66
Be	255	85	S	3	1	Mo	1	0.33
Bi	274	91.33	Sb	119	39.6	Na	8	2.66
Cd	265	88	Sc	2	0.66	Nb	268	89.3
Co	2	0.66	Se	206	68.6	Tl	296	98.6
Ga	101	33.6	Sn	293	97	U	292	97.3
Ge	213	71	Ta	300	100	W	264	88
Hg	100	33.33	Te	283	94.3	Zr	118	39.3

4.3. The Isometric Log-Ratio EM Algorithm (ilr-EM)

This method was introduced by Fernández et al. in 2012. Its primary goal is to reduce the impact of outliers on imputed values. This method is based on a multivariate normal model applied to ilr-transformed

data. The ilr transformation for a D-part composition $X_i = [x_{i1}, \dots, x_{iD}], i = 1, \dots, n$ is defined by Equation 6, and the inverse ilr transformation is given by:

$$\begin{cases} x_{1i} = exp\left(-\sqrt{\frac{D-1}{D}} z_n\right) \\ x_{ij} = exp\left(\sum_{i=1}^{j-1} \frac{1}{\sqrt{(D-l+1)(D-1)}} z_n - \sqrt{\frac{D-j}{D-j+1}} z_{ij}\right) \\ x_{iD} = exp\left(\sum_{i=1}^{D-1} \frac{1}{\sqrt{(D-l+1)(D-1)}} z_n\right) \end{cases} \quad (6)$$

This method relies on a censored robust regression model. The algorithm's steps can be summarized as follows:

1. Select an element (x_j) with missing values and perform its ilr transformation based on Equation 3-4.
2. Use Equation 7 to apply the censored robust regression of z_1 on $z_{D-1}, \dots, z_2$ to estimate missing cells, and repeat the EM scheme until convergence.

$$\hat{y}_{ij} = y_i^t \hat{\beta}_j^{(k)} = \hat{\sigma}_j^{(k)} \frac{\emptyset\left(\frac{\psi_{ij} - y_{ij}^t \hat{\beta}_j^{(k)}}{\hat{\sigma}_j^{(k)}}\right)}{\Phi\left(\frac{\psi_{ij} - y_{ij}^t \hat{\beta}_j^{(k)}}{\hat{\sigma}_j^{(k)}}\right)} \quad (7)$$

where y_{ij}^t is the transposed vector of observed values (after ilr transformation), $\hat{\beta}_j^{(k)}$ is the vector of regression coefficients estimated in the k-th iteration, σ_j^2 is the conditional variance estimate of the variable y_j in k-th iteration, ψ is the detection limit vector after ilr transformation, and ϕ and Φ are the standard normal density and cumulative distribution functions, respectively.

3. Perform the inverse transformation using Equation 3-6.
4. Repeat steps 1 to 3 for all variables with missing values.

This method is available in the R software package "zCompositions" [25].

Based on Table 1, the elements Hg, Ga, Zr, Sb, Rb, Th, Ag, Se, Ge, Be, W, Cd, Nb, Bi, Te, Sn, U, Tl, and Ta were excluded from the dataset due to significant censored data. The remaining censored values in other elements were imputed using the ilr-EM algorithm. The statistical parameters of the elements after replacing censored values are provided in Table 2.

4.4. Univariate Analysis

In almost all statistical methods used in geochemistry, the goal is to detect apparent anomalies (abnormal values in the population) during geochemical exploration. These methods are classified into two categories based on the number of variables considered: univariate and multivariate. In univariate methods, the variations and parameters of each variable are analyzed separately, and the results are presented as maps after performing various analyses. One of the ways to understand the relationships between data and information in an exploration project is through map plotting. Maps are the result of data processing, analysis, and appropriate estimation, providing significant assistance in understanding relationships between components, interpreting results, and ultimately optimizing the design for the next phase.

Univariate anomaly separation methods are typically divided into two main categories: structural and non-structural methods. Non-structural methods determine threshold limits based on distribution

parameters, while structural methods also consider the spatial structure and relationships of samples to determine threshold limits.

For univariate statistical analysis, the dataset was unfolded using the central log-ratio (clr) transformation. Exploratory Data Analysis (EDA) graphs of the variables before and after clr transformation for the elements Cu, Au, and Mo are shown in Figs. 3 to 5.

Table 2. statistical parameters of the elements after replacing censored values (PPM & Au in PPb).

Element	Min	Q1	Median	Mean	Q3	Max
Al	0.2	1.228	3.79	4.152	6.81	9.51
As	1.805	9	19	44.326	45.25	1267
Au	0.00478	0.02	0.075	0.17499	0.21	2.5
B	0.08392	0.4182	0.7346	2.92951	2.1327	27
Ba	12	102.8	238	312.7	439.2	1727
Ca	0.22	1.683	3.735	4.356	6.32	14.6
Ce	3	24	31	30.97	37	64
Co	0.8439	10	13	14.4591	16.25	71
Cr	2	9	13	68.05	46.25	770
Cu	3	117	329	674.8	1003.5	4778
Fe	2.3	3.797	4.45	4.795	5.303	14.4
K	0.02	0.25	0.55	0.9048	1.38	5.26
La	1.699	14	17	17.506	21	41
Li	1.123	7	20	19.586	27	78
Mg	0.04	0.5275	1.155	1.4618	2.04	9.39
Mn	46	430.5	680	836.8	1090.2	9122
Mo	0.8389	7	12	19.5561	23	290
Na	0.00233	0.03	0.09	0.51505	0.28	5.14
Ni	0.6536	5	11	50.435	32	639
P	0.014	0.0678	0.1055	0.10548	0.1365	0.23
Pb	1.72	9	13	38.83	22	3612
S	0.00586	0.04	0.08	0.23837	0.21	3.42
Sc	0.5544	6	8	8.9179	11	31
Sr	27	104	188	247.3	317.5	970
Ti	18	166	1851	1733	2777	10713
V	6	70	97	101	128.2	251
Zn	4	43	61	96.08	97	2806

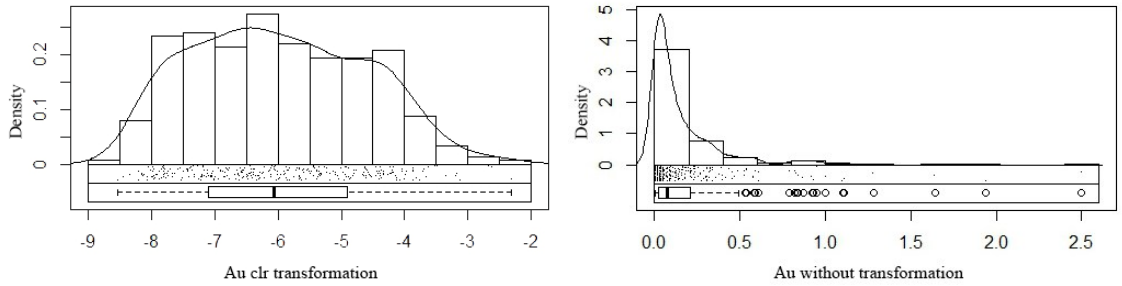

Fig. 3. EDA Plot for Au Before (Right) and After (Left) clr Transformation.

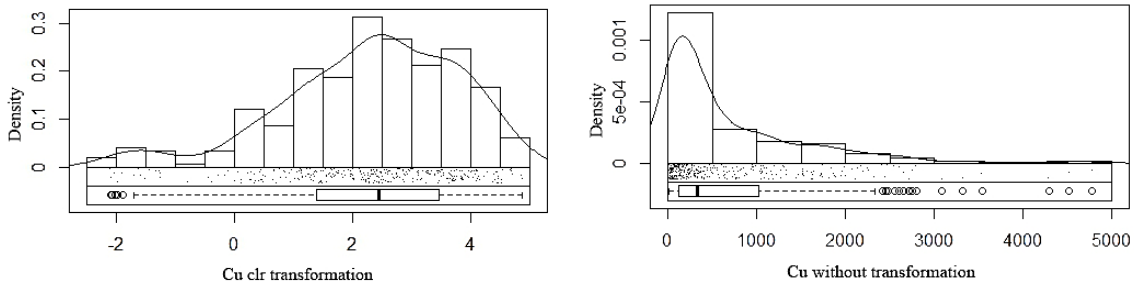

Fig. 4. EDA Plot for Cu Before (Right) and After (Left) clr Transformation.

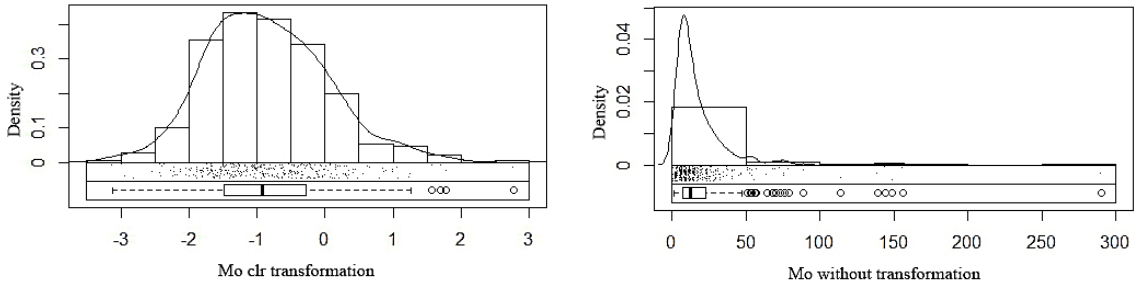

Fig. 5. EDA Plot for Mo Before (Right) and After (Left) clr Transformation.

Correlation between elements cannot be defined in a closed environment since such coefficients may arise due to the closed nature of the data. The data must first be opened before calculating element correlations. When the clr transformation is used to open the data, the correlation coefficient corresponds to the geometric mean of the variables in the samples. Since there is no issue of variable selection, the clr transformation is preferred for correlation coefficient analysis. Fig. 6 illustrates the correlation of several mineralization-related elements opened by the clr transformation.

In Fig. 6, after applying the Centered Log-Ratio (CLR) transformation, which is used to mitigate the effects of compositional closure in geochemical data, the distribution of elements has become closer to normal. The results of this analysis reveal a high correlation between nickel (Ni) and chromium (Cr), likely due to a common magmatic origin or related geological conditions. These elements are often associated with mafic and ultramafic rocks in geochemical processes and may have been introduced simultaneously into the environment through shared magmatic or alteration processes. Additionally, in ultrabasic rocks, Ni

and Cr typically concentrate in minerals such as spinels and olivine, explaining the strong correlation observed. In porphyry systems, elements like lead (Pb) and zinc (Zn) are recognized as supergene enrichment indicators, often concentrated near the Earth's surface during the final stages of mineralization.

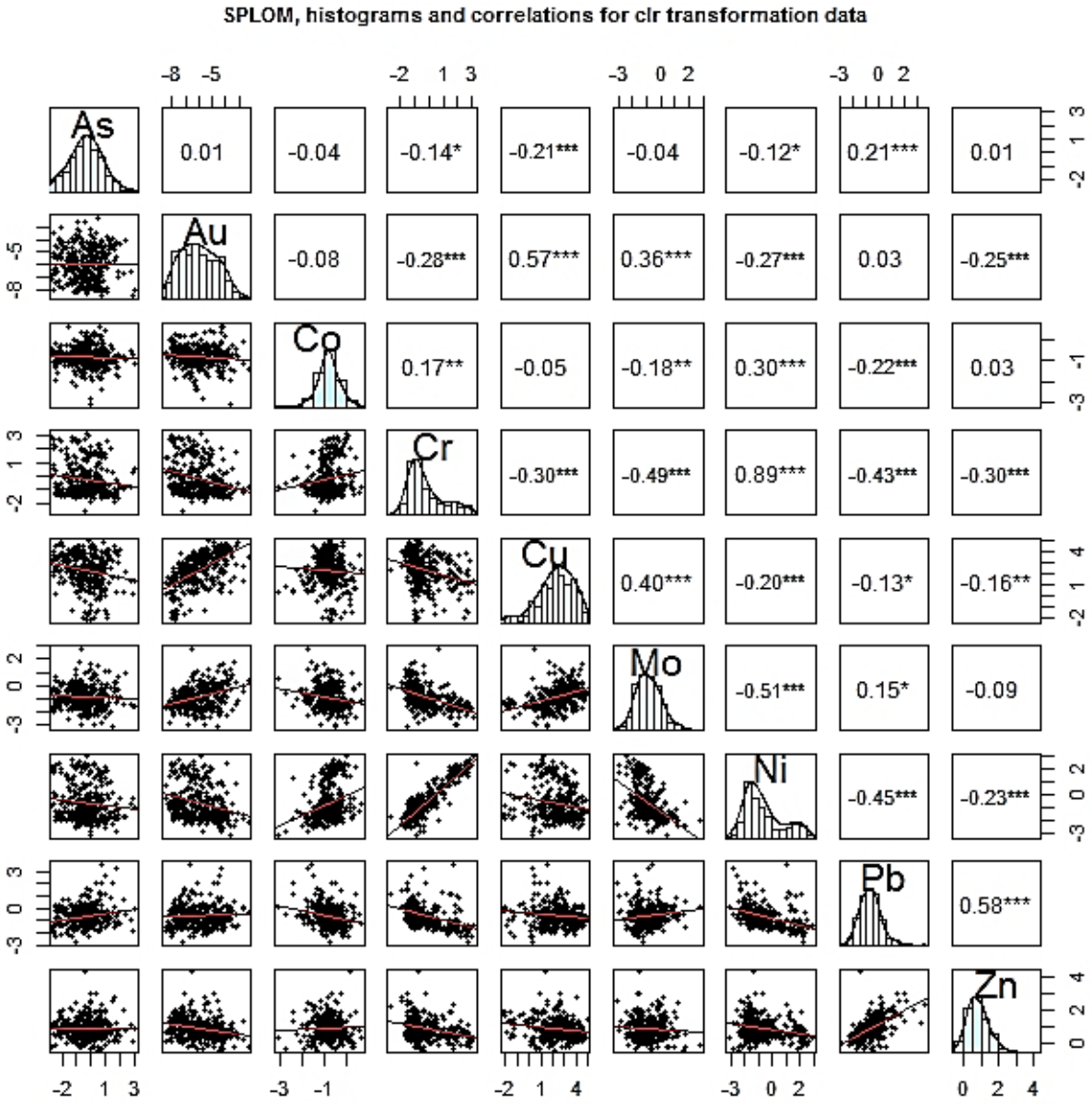

Fig. 6. Scatter Plot, Histogram, and Pearson Correlation of Some Mineralization-Related Elements After clr Transformation.

These elements are typically found in the upper zones of hydrothermal systems, often in association with Cu sulfides and other base metals. The high correlation between Pb and Zn suggests a mineralization phase in the Shadan porphyry system, wherein these elements accumulate near the surface, potentially due to secondary mineralization processes. Au (Au), Cu (Cu), and Mo (Mo) show a strong correlation, which is characteristic of porphyry-style mineralization and is linked to deeper hydrothermal zones. This correlation likely reflects the involvement of these elements in primary mineralization processes, influenced by hydrothermal fluids originating from magmatic intrusions. In porphyry systems, Cu and Mo are key

indicators of mineralization, and the concurrent presence of Au may be attributed to specific physicochemical conditions, such as pressure and temperature changes or the composition of hydrothermal fluids. Overall, these positive correlations highlight the role of magmatic and hydrothermal processes in enriching the area with these elements, which is consistent with the presence of porphyry systems and alteration zones in the Shadan region.

To distinguish anomalies from the geochemical background for Cu, Au, and Mo, the concentration-area fractal method has been applied, as discussed in the following sections.

4.5. Concentration-Area Fractal Method

The concentration-area fractal method is one of the common techniques used to separate geochemical anomalies from the background. The spatial distribution of most elements in a given geological-geochemical environment is the end product of various geological events such as volcanic activity, intrusive bodies, sedimentation, tectonics, and mineralization. During these events or processes, certain elements become enriched and potentially form ore-grade materials, while others become dispersed. The spatial characteristics displayed by elements related to mineralization provide guidelines for exploration activities. Given that mineralized populations arise from different processes than those generating the background, one can expect them to exhibit distinct spatial distribution and morphological characteristics. One such characteristic is the fractal dimension of geochemical data. Fractal dimensions, which are typically non-integer values, can be used to express the complexity of a shape or distribution. Various fractal-based methods have been developed, such as concentration-area, concentration-perimeter, concentration-distance, and power spectrum-area methods. Among these, the concentration-area method has found widespread application in geosciences.

The concentration-area (or Concentration-Area) fractal method was initially proposed by Cheng et al. in 1999 to examine the characteristics of geochemical patterns. Variants of this method, such as the concentration-distance and power spectrum-area methods, have also been developed, all of which have produced satisfactory results when analyzing geochemical data in landscapes with fractal properties. In general, the concentration-area fractal method is considered a fundamental technique for modeling geochemical anomalies.

This method is based on fractal theory, which analyzes the natural complexity and anomalies in data using self-similarity properties. In the concentration-area method, the spatial distribution of elements in the studied geological environment is examined, and a relationship between the concentration (grade) of an element and the cumulative area of regions with that concentration is established. Based on this relationship, elements are classified into two general groups: background and anomalies. This classification is based on an exponential model, which states that the area of regions with concentrations lower than or equal to a particular threshold decreases exponentially with the grade of the element. To apply this method, the spatial distribution of a specific element is first analyzed, and the area of regions with particular concentrations is calculated. Then, the relationship between the logarithm of concentration (grade) and the logarithm of the cumulative area is plotted. The resulting graph typically displays straight lines, each representing a distinct geochemical population. The intersection points of these exponential lines are defined as threshold values that clearly distinguish between background and anomaly populations. In other words, this method systematically separates anomalous regions (populations with concentrations above the threshold) from the background regions (populations with concentrations below the threshold). This enables the rapid and accurate identification of regions with high mineral potential. The primary advantage of this method is its simplicity and high efficiency, as it does not require complex data processing or smoothing filters and works directly with raw data. Consequently, the concentration-area method is one of the most widely used techniques in exploration geology, providing reliable results for identifying geochemical anomaly areas.

Given that the focus of this study is on Cu, Au, and Mo mineralization within the study area, the concentration-area fractal method was applied to the CLR-transformed data for these elements using the "rgr" package in R. The logarithmic plots of concentration and cumulative area pairs for each element are presented in Figs. 7 to 9. Each straight line represents a population, and the intersection points of these lines

indicate the threshold that separates background and anomalous populations or their subsets. Based on the breakpoints of the lines in the graphs, the threshold values for the elements were determined, as shown in Table 3. Using these thresholds, the anomaly and background maps were subsequently generated.

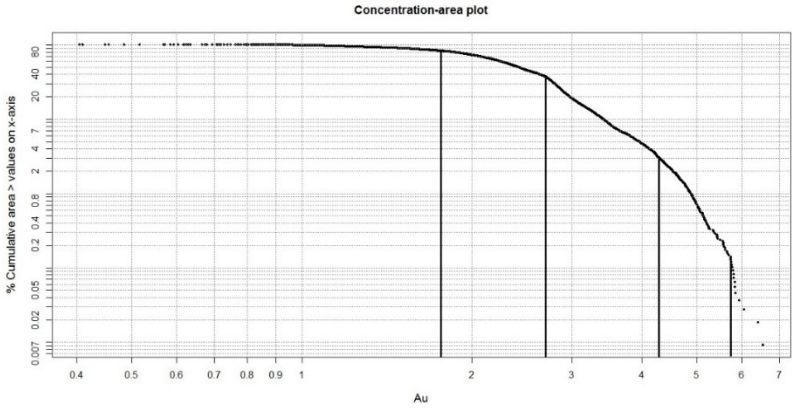

Fig. 7. Logarithmic Concentration-Area Plot for Au (ppb).

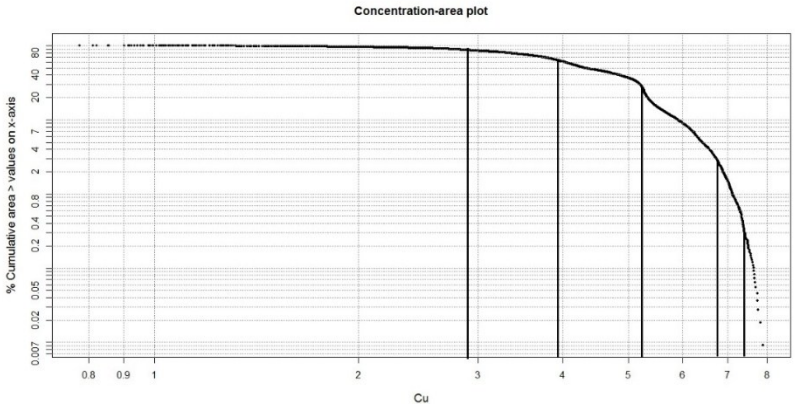

Fig. 8. Logarithmic Concentration -Area Plot for Cu (ppm).

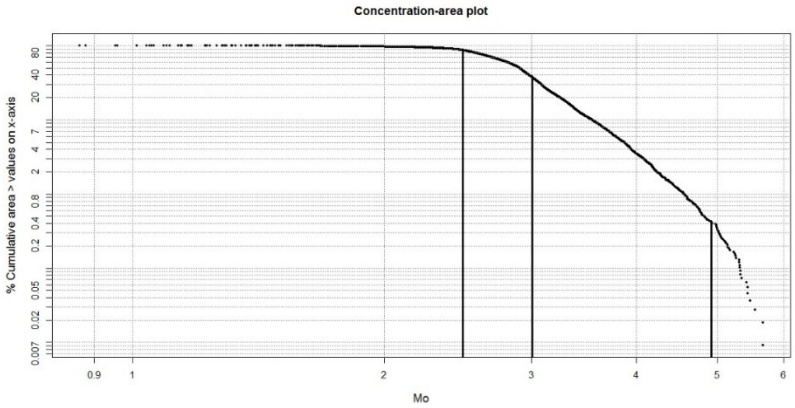

Fig. 9. Logarithmic Concentration -Area Plot for Mo (ppm).

Table 3. Thresholds obtained from the Concentration -Area Plot.

Element	Threshold 1	Threshold 2	Threshold 3	Threshold 4	Threshold 5
Au	-6.99126	-6.15	-4.99	-3.98	
Cu	0.0078	1.0286	2.0077	3.8227	4.531
Mo	-1.486	-0.999	1.0011		

The Au, Cu, and Mo mineral anomalies in the study area are primarily associated with quartz diorite to granodiorite intrusive rocks, locally referred to as the "Shadan porphyry." These rocks, considered intermediate intrusive igneous rocks, typically serve as suitable hosts for hydrothermal mineralization, particularly porphyry systems. In this region, Au and other metal anomalies are predominantly situated within these intrusive bodies, indicating a genetic relationship between magmatic processes and mineralization. In the northwestern part of this anomaly, Au mineralization occurs adjacent to the main intrusive body within a silicified-carbonate shear vein. These veins, known as "silicified-carbonate breccias," represent fractured structures filled with minerals, often formed by tectonic activities and the passage of hydrothermal fluids. In such systems, solutions containing metallic elements, including Au, along with silica and carbonate, penetrate the fractures in the host rocks, resulting in the deposition of minerals, particularly along the newly formed veins. This type of vein mineralization is a key characteristic of hydrothermal zones with intense alteration. In porphyry systems, these veins and breccias typically act as primary conduits for the transport of ore-bearing fluids and have significant potential for hosting Au deposits. The Cu and Mo anomalies exhibit a similar pattern. In these areas, the anomalies are frequently associated with quartz diorite to granodiorite rock units and silicified-carbonate breccia veins. This indicates that Cu and Mo mineralization occurs disseminated within the intrusive bodies and is concentrated in hydrothermal fractures. In porphyry systems, Cu and Mo typically form as a result of hydrothermal alteration associated with intrusive bodies, particularly in dioritic and granodioritic units. In this process, hot fluids containing these metals separate from the magma and migrate upwards through fractures and shear zones, where the deposition of these elements occurs. Therefore, the geochemical association between Au, Cu, and Mo anomalies with intrusive igneous bodies and silicified-carbonate breccia systems in this area supports the presence of a large porphyry system (Figs. 10 to 12).

During the geochemical data analysis, to enhance accuracy and reduce complexity in interpretation, the removal of certain elements is essential. This is achieved through a thorough understanding of the lithological units and their rock-forming compositions. In this context, elements such as aluminum (Al), calcium (Ca), iron (Fe), potassium (K), magnesium (Mg), sodium (Na), phosphorus (P), sulfur (S), cerium (Ce), and lanthanum (La) have been excluded from the dataset, for important geochemical reasons. These elements, known as "rock-forming elements," are typically abundant in most lithological units and play a crucial role in forming and stabilizing mineralogical structures in the rock units. Due to their high abundance in various rocks, their presence usually does not have a direct correlation with economic mineralization processes. In other words, these elements are often part of the background matrix and have little relevance to identifying anomalies related to economic mineralization. Geochemical analyses are primarily conducted to identify anomalies related to economic mineralization. By excluding background elements, the focus shifts towards elements such as Cu (Cu), Au (Au), Mo (Mo), lead (Pb), zinc (Zn), and other key elements associated with economic mineralization. These elements, often present in mineralized zones, can provide important geochemical clues.

After excluding the rock-forming elements, the remaining data for 17 elements are subjected to multivariate analysis.

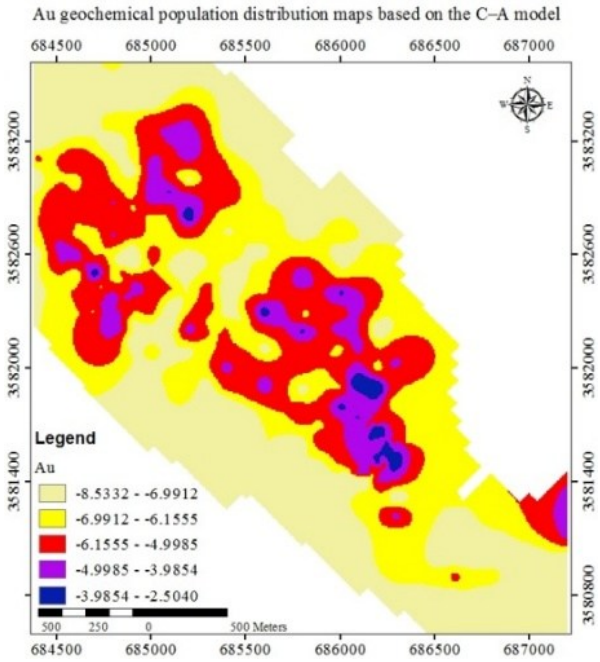

Fig. 10. Geochemical Community Distribution Map for Au Based on Fractal Concentration -Area Geometry.

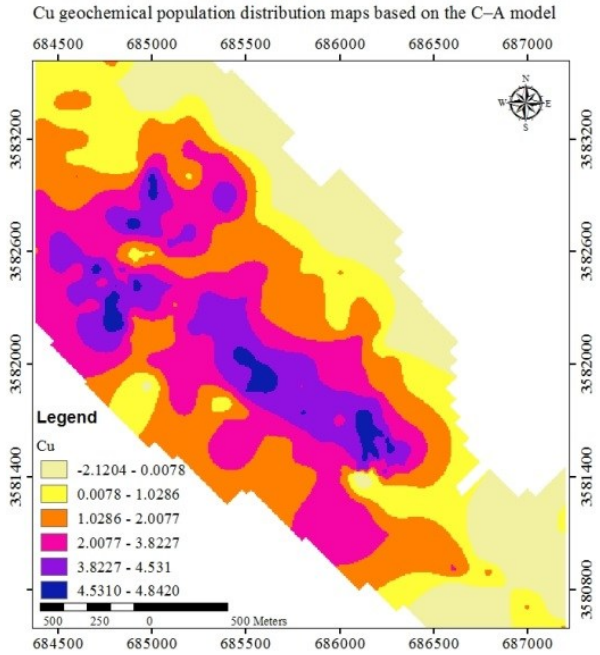

Fig. 11. Geochemical Community Distribution Map for Cu Based on Fractal Concentration -Area Geometry.

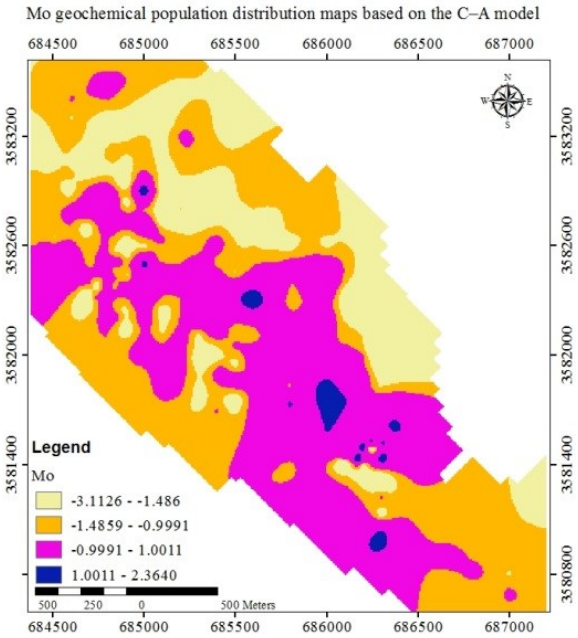

Fig. 12. Geochemical Community Distribution Map for Mo Based on Fractal Concentration -Area Geometry.

4.6. Robust Factor Analysis

Experience has shown that when a combination of variables is used instead of a single variable, the ability to detect composite geochemical halos around ore-bearing intrusions and identify anomalies related to mineralization increases significantly. Moreover, random errors in using a combination of variables are reduced. Factor analysis is one of the most important multivariate statistical methods, widely used for preprocessing and dimensionality reduction of data, and the resulting components are employed for multivariate statistical analyses [8, 26]. The robust factor analysis (PFA) method is a statistical technique used to identify hidden structures within a set of variables. The goal of this method is to reduce the number of variables to a few factors that can explain most of the variability in the data. This method models the observed variables as a combination of several latent variables (factors) and an error component, simplifying the complex structure of the data.

The main model in factor analysis is expressed in equations, where each observed variable X_i is defined as a linear combination of latent factors f_j and error components e_i. In matrix form, the general model is as follows:

$$[X] = [\mu] + [A][f] + [e] \quad (8)$$

- [X]: Vector of observed (measured) variables.
- [μ]: Vector of variable means.
- [A]: Factor loading matrix, indicating the influence of each factor on the observed variables.
- [f]: Vector of factors, representing the latent variables.
- [e]: Vector of errors, representing the difference between the observed and predicted variables by the factors.

In this model, the goal is to find the coefficient matrix [A] that explains the most variability in the data. To achieve this, factor analysis is based on the covariance or correlation matrix of the observed variables:

$$\sigma^2[I] + T[A][A] = [S] \quad (9)$$

Where:

- [S]: Covariance matrix of the observed variables.
- σ^2 [I]: Error component, representing the variability due to random factors or measurement errors.

To find the coefficient matrix [A], the principal component analysis (PCA) method is used. In this method, the covariance matrix of the original variables is calculated, and then the eigenvalues and eigenvectors of this matrix are obtained. The eigenvectors represent the principal factors, and the eigenvalues indicate the amount of variability explained by each factor. To select the appropriate number of factors (k factors), typically, factors with larger eigenvalues are chosen, as they explain most of the data's variability. This selection is usually made using a Scree plot, which shows which factors contribute most to explaining the variations. One of the main challenges in classical factor analysis is its sensitivity to outliers. Outliers can significantly distort the results of the analysis because their unique nature affects the correlation structure of the data. Therefore, in robust PFA, methods are used that are less sensitive to these outliers. One such method is the Minimum Covariance Determinant (MCD). In this method, instead of using the classical covariance matrix, a subset of data is selected in which the determinant of the covariance matrix is minimized, reducing the influence of outliers. To identify outliers, the Mahalanobis distance is used. The Mahalanobis distance is a measure of the distance of each observation from the center of the data distribution in a multivariate space. For multivariate normal data, this distance follows a chi-square distribution. Thus, outliers are identified by comparing the Mahalanobis distance to chi-square values. If outliers are present, the chi-square plot, which should be linear, will deviate. In conclusion, this robust approach (PFA using MCD) was specifically applied to the geochemical data from the Shadan region. By using this method, the data were analyzed with greater accuracy, and outliers were identified and removed, resulting in more precise outcomes in the analysis of mineralization and geological features of the region [3, 8, 12, 19].

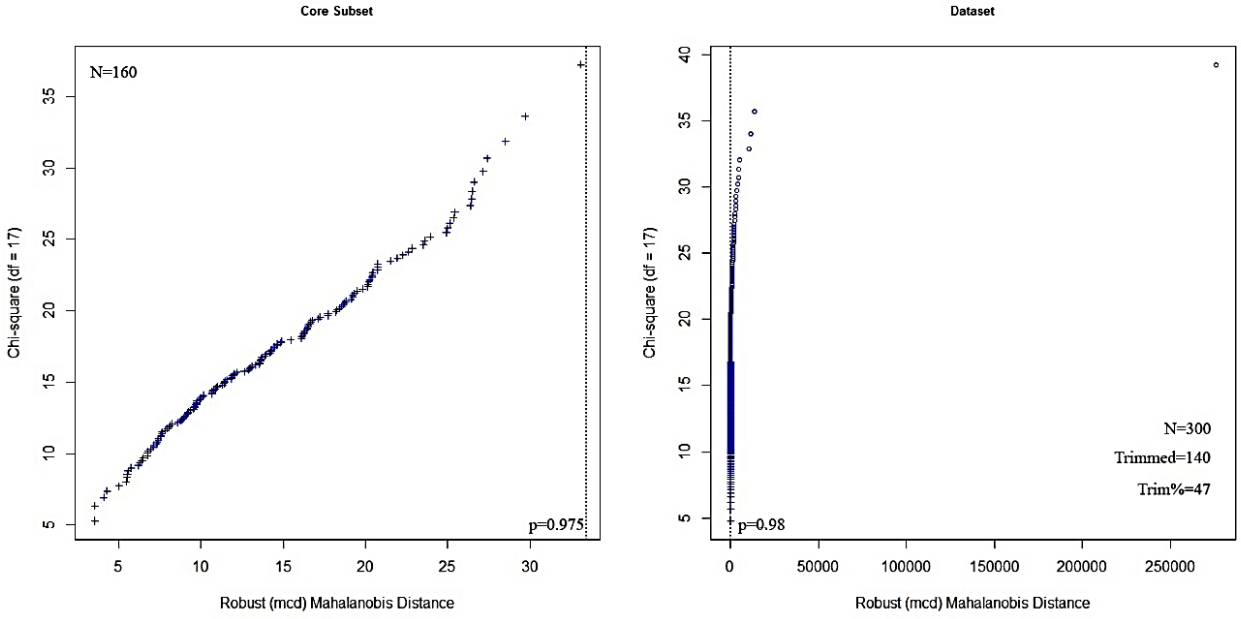

Fig. 13. Outliers and Core Compositions Used in the Analysis.

Fig. 13 illustrates the geochemical data analysis of the Shadan area using Mahalanobis distance and chi-square distribution to identify outliers. The left chart, "Core Subset," shows the primary samples that, after removing outliers, align along a nearly straight line according to the chi-square distribution (with 17 degrees of freedom). This line indicates the data's conformity to a normal distribution. Additionally, the tail regions of the plot, which deviate from the straight line, suggest the presence of samples with higher Mahalanobis

distances, indicating potential outliers. In the right-hand plot, which represents the entire dataset, Mahalanobis distances for all 300 samples are displayed, clearly revealing the outliers. Specifically, data points located to the far right of the plot, with significantly high Mahalanobis distances, are identified as outliers. Here, 140 samples (47% of the total) were excluded due to their extremely high values. This analysis demonstrates that the MCD (Minimum Covariance Determinant) method successfully separated the core and primary data from the outliers, and the remaining data conforms to a normal distribution. By removing these outliers, a robust covariance matrix was generated, which more accurately reflects the true correlations among the data and prevents distortion caused by anomalous data points.

After identifying the outliers, a robust factor analysis was performed using varimax rotation on the extracted components. To interpret the variables, the factor loadings in the analysis were transformed from the isometric log-ratio (ilr) space back to centered log-ratio (clr) space. According to the Scree Plot, presented in Fig. 14, four main components were selected, collectively explaining 75% of the variability in the region's data. The selection of these four components was done in a controlled manner based on the results of the analysis.

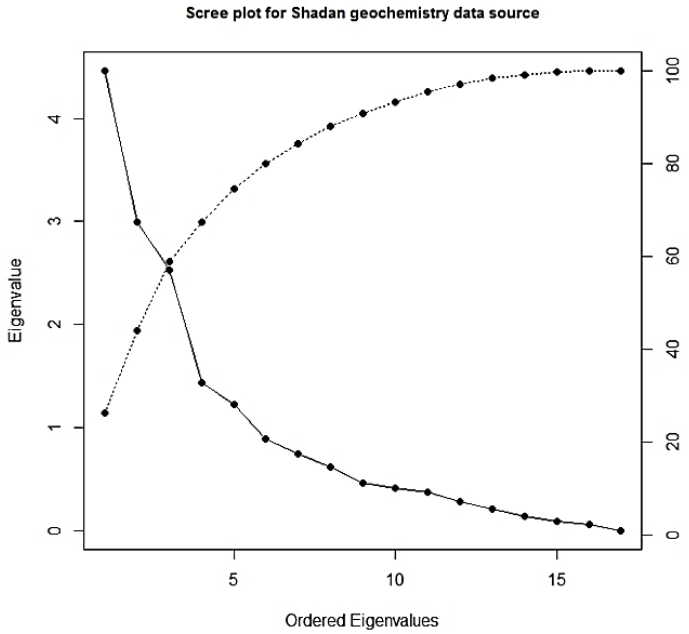

Fig. 14. Scree Plot of RPFA Analysis of Compositional Data.

The biplot from the robust principal component analysis (PCA) is provided in Fig. 15. The factor loadings from the robust factor analysis, considering a minimum loading value of 0.5, are shown in Fig. 1.

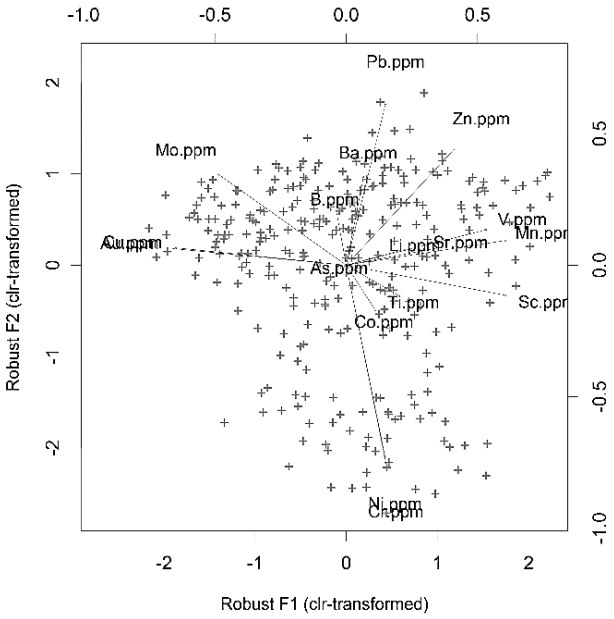

Fig. 15. Biplot Constructed Using clr-Transformed Data.

The biplot, plotted using clr-transformed data, demonstrates that the compositional nature of the data, which often leads to biases and errors in interpretation, has been mitigated through this approach. Furthermore, the use of robust analysis minimized the impact of outliers and provided a more accurate representation of the true correlations among the data. The two-dimensional biplot depicts the result of the robust factor analysis on geochemical data transformed via the clr method. This analysis focuses on two main factors, F1 and F2, which account for a significant portion of the data's variability. Elements close to each other on this plot exhibit high correlations and have likely participated in similar geological or mineralization processes. For instance, lead (Pb) and zinc (Zn), which are situated near each other, likely indicate participation in similar hydrothermal mineralization systems. Additionally, Cu, Mo, and Au, which are grouped, demonstrate a close relationship in economic mineralization zones associated with porphyry systems. Elements located farther from the origin of the plot play a more prominent role in explaining data variability. For example, Au, positioned on the left and distant from the origin, highlights its importance in economic mineralization. Conversely, vanadium (V) and manganese (Mn), located on the right side of the plot, contribute significantly to the second factor. The direction of the vectors indicates positive or negative correlations among the elements. For instance, a negative correlation between Cu and Mo with lead and zinc is observed, suggesting differing geochemical conditions or mineralization environments. Arsenic (As), located near the center of the plot, exhibits weaker correlations with other elements but may still play a role in certain mineralization zones.

The elements grouped within each factor are linked to specific geological and geochemical processes that occurred during the geological evolution of the region. This combination of elements reflects the geological and geochemical relationships between them, and the reason for their co-occurrence can be attributed to different geological processes [3, 8]. The first factor, explaining 30% of the total data variability, shows positive loadings for manganese, scandium (Sc), and vanadium, and negative loadings for Au, Cu, and Mo. These negative loadings indicate geochemical characteristics associated with Au, Cu, and Mo mineralization, which point to significant mineral zones in the region.

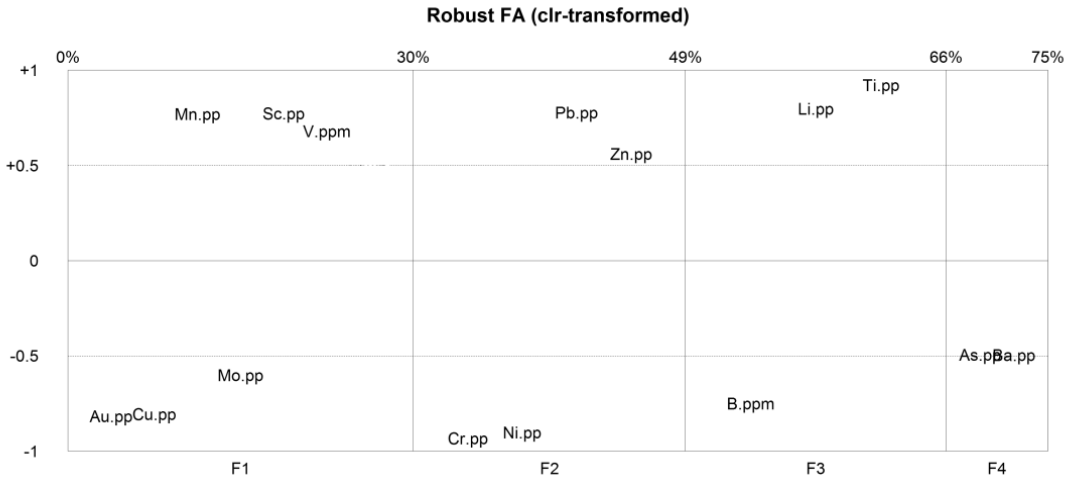

Fig. 16. Loads Greater than 0.5 in Different Components of the RPFA Analysis of Compositional Data.

Mn, Sc, and V are generally associated with mafic and ultramafic rocks and may have concentrated during specific alteration processes, whereas Au, Cu, and Mo are linked to hydrothermal systems and deep mineralization zones such as porphyry deposits. The second factor, accounting for 19% of the data variability, has positive loadings for lead and zinc and negative loadings for chromium (Cr) and nickel (Ni). Lead and zinc are known as supergene elements and typically appear in hydrothermal and porphyry systems, where they are transported via hydrothermal fluids to shallower zones and accumulate in carbonate or alteration rocks. On the other hand, chromium and nickel are associated with mafic and ultramafic origins, commonly found in mafic igneous rocks like peridotite and chromite. This contrast between Pb-Zn and Cr-Ni groups points to their differing geochemical origins, with lead and zinc indicative of hydrothermal processes, while chromium and nickel stem from igneous origins. In the third factor, which explains 17% of the data variability, lithium (Li) and titanium (Ti) show positive loadings, while vanadium has negative loadings. Lithium typically concentrates in hydrothermal and alteration environments, while titanium is found in resistant minerals such as rutile and ilmenite. Vanadium is found in mafic and ultramafic rocks and iron-bearing minerals. The contrast between these elements indicates differences in the geological and geochemical processes that influenced each of them. Lithium and titanium are linked to hydrothermal alteration, while vanadium is more related to igneous processes. The fourth factor, which explains 9% of the total variability, includes negative loadings for arsenic and barium (Ba). These elements are often considered indicators of hydrothermal environments and are commonly present in sulfide and epithermal mineralization zones. Arsenic accumulates widely in deep hydrothermal zones, and barium appears in barite minerals under hydrothermal conditions. This factor reflects zones enriched with elements related to hydrothermal systems, which are important markers in geochemical surveys for identifying mineralization zones. As a result, the grouping of elements within each factor is due to their distinct geochemical origins and geological processes that have influenced the Shadan area. Elements associated with hydrothermal mineralization, such as Au, Cu, and Mo, are grouped, while elements associated with mafic and ultramafic rocks, such as Cr and Ni, are found in another factor. This clear separation demonstrates that different tectonic and geochemical processes have played a role in the formation of the area's mineralization.

The first factor, with negative loadings, highlights the geochemical characteristics of Cu, Au, and Mo mineralization. Other factors are related to the enrichment of supergene elements, marginal mineralization characteristics, and geochemical features of siderophile elements, as well as the nature of the sampling environment. The overall conclusion from these analyses is that the Shadan area has been influenced by multiple, complex geological and hydrothermal processes, resulting in the geochemical concentration and segregation of various elements. This data indicates that the main mineralizations in the region, particularly related to Cu, Au, Mo, lead, and zinc, are associated with deep hydrothermal systems and active geological processes, signifying high mineral potential.

Previously, the concentration-area fractal method was applied to construct geochemical maps based on univariate analysis. In this study, the concentration-area method has also been used to classify the map derived from factor scores of the first factor. It is worth noting that since the Au, Cu, and Mo elements showed high negative loadings in the first factor, the factor scores have been multiplied by -1 to facilitate comparison of the final map for this component.

The logarithmic plots of Concentration-Area pairs and cumulative area thresholds for the first factor scores have been obtained and are presented in Fig. 17 and Table 4.

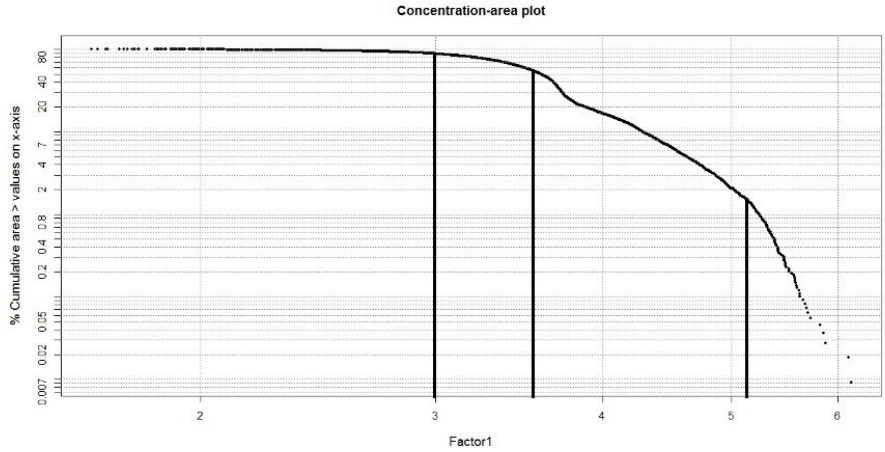

Fig. 17. Logarithmic Factor Score-Area Plot for Factor 1 scores.

Table 4. Thresholds Obtained from the Concentration-Area Method for Factor Scores of the First Factor.

	Thresholds 1	Thresholds 2	Thresholds 3
Factor1	-0.98525	-0.5995	1.1453

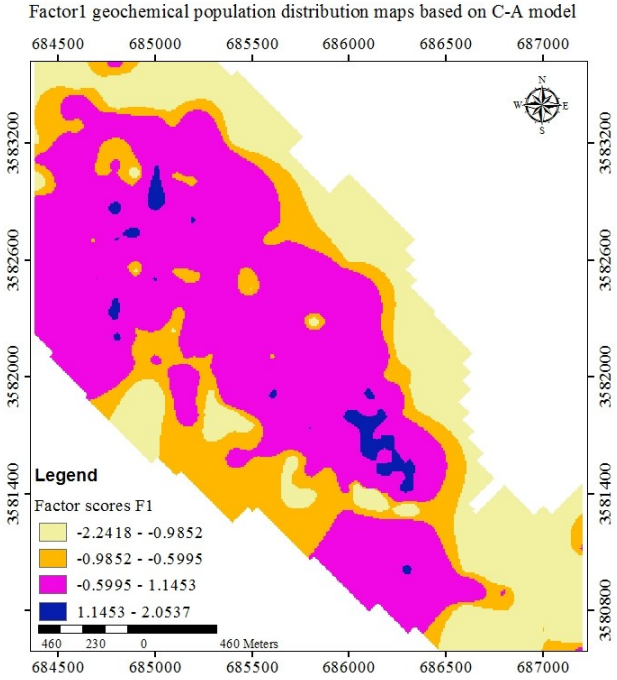

Fig. 18. Geochemical Community Distribution Map of Factor Scores for the First Factor Based on Fractal Concentration -Area.

Based on the anomaly derived from the first factor scores (for Cu, Au, and Mo) (Fig. 18) and the geological map of the region, the anomaly is primarily concentrated on the quartz diorite to granodiorite intrusive bodies (known as the Shadan porphyry). These intrusions, typically associated with porphyry systems, host hydrothermal mineralizations. Au, Cu, and Mo mineralization in this region occurs within silicified-carbonate breccia veins, indicating the concentration of metals within vein and breccia systems with hydrothermal alteration. This pattern generally suggests the high mineral potential of the area for metal deposits.

5. Discussion

The geochemical anomalies derived from the data in the Shadan region indicate a strong correlation between nickel (Ni) and chromium (Cr). This correlation may result from a similar magmatic origin or related geological conditions. Nickel and chromium are typically found together in mafic and ultramafic rocks, which are usually composed of minerals like spinel and olivine, stable under high temperature and pressure conditions. These two elements are separated from the magma during early magmatic processes and are transported to the surface through hydrothermal processes. Nickel and chromium concentrate in these minerals, which could explain their strong correlation. In magmatic and alteration systems, the simultaneous transport of these elements, due to their similar chemical properties, results in a high correlation between them. Additionally, in ultrabasic rocks, nickel and chromium often concentrate in spinel and olivine minerals, which are considered primary reserves of these elements. This indicates that mafic and ultramafic rocks in the region could be the primary source of these elements. In mafic rocks, hydrothermal processes introduce these elements into magmatic systems, resulting in nickel and chromium minerals being deposited in specific zones of intrusive rocks [27].The data analysis also reveals a strong correlation between Pb and Zn. These two elements are typically concentrated in the supergene zones of porphyry systems. In these systems, lead and zinc are recognized as elements associated with the final

stages of mineralization and are usually found in the upper zones of hydrothermal systems. In these zones, changes in pressure and temperature conditions cause hydrothermal solutions containing these elements to precipitate. In porphyry systems, lead and zinc, due to their role in late mineralization processes, usually accumulate near the surface along with Cu sulfides and other base metals. The strong correlation between these two elements may be due to their presence in a specific mineralization phase following secondary mineralization processes in which lead and zinc precipitated under specific physico-chemical conditions [28]. The data also show a high correlation between Au, Cu, and Mo. These three elements are considered key indicators of mineralization in porphyry systems. Porphyry systems typically host hydrothermal mineralization processes, and due to the influence of magmatic bodies and the hydrothermal fluids generated by them, Cu, Au, and Mo mineralization occurs simultaneously in these systems. In these systems, Mo often concentrates in the core of the porphyry system, while Cu and Au are concentrated in the peripheral zones. Variations in pressure and temperature, as well as the chemical composition of the hydrothermal solutions, determine the location and amount of deposition of these elements. Au, Cu, and Mo mineralization occur primarily at greater depths in porphyry systems, where conditions are optimal for the deposition of these elements. Au is usually transported along with Cu and Mo in hydrothermal solutions and is concentrated in shear zones and fractures under the influence of hydrothermal alteration processes. The simultaneous presence of these three elements in the studied region indicates that magmatic processes are responsible for their distribution and concentration. In these systems, changes in physico-chemical conditions, particularly during magmatic and alteration processes, play a key role in determining the composition and concentration of these elements [28, 29]. Furthermore, geochemical and geological data indicate that the Au, Cu, and Mo anomalies are mainly associated with quartz diorite to granodiorite intrusive bodies. These intrusions, known as the "Shadan porphyry," consist of intermediate intrusive igneous rocks that typically serve as suitable hosts for hydrothermal mineralization. Porphyry systems in these types of intrusive igneous rocks are often rich in metallic elements, including Au, Cu, and Mo, due to the interaction between hydrothermal fluids and shear or fracture zones. In the northwestern part of the anomaly, Au mineralization occurs near the main intrusive body in a silicified-carbonate breccia vein. These types of veins, formed by tectonic activities and hydrothermal fluid flow, act as main pathways for the transport of metallic solutions and Au accumulation. Hydrothermal solutions, which flow through fractures and shear zones during these processes, enter these structures along with silica and carbonate, leading to the precipitation of Au. Au mineralization in these types of shear veins indicates strong hydrothermal activity in this region, which has a significant impact on the concentration of precious metals. Cu and Mo mineralization also follows a similar pattern. In these areas, Cu and Mo mineralization often occurs in association with quartz diorite to granodiorite units and silicified-carbonate breccia veins. This suggests that dioritic and granodioritic intrusive bodies acted as the main sources of hydrothermal fluids rich in Cu and Mo. The hydrothermal solutions, separated from the magmatic bodies and migrating towards the surface, reached areas on the Earth's surface where these elements precipitated through fracture and shear systems [30]. The geochemical and geological data analysis, particularly the correlations between metallic elements and geological structures, indicate that the Shadan region holds significant potential for Au, Cu, and Mo mineral exploration. The accumulation of these elements in porphyry systems and silicified-carbonate breccia veins suggests that this region has been subjected to extensive magmatic and hydrothermal processes. Therefore, it can be considered a large porphyry system with substantial metallic deposits.

6. Conclusion

The analysis of 300 rock samples from the Shadan region revealed significant concentrations of Cu (up to 0.47%) and Au (up to 2.5 g/t), highlighting the region’s strong potential for both base and precious metal mineralization. Multivariate analysis using ILR transformation and robust factor analysis identified four major geochemical components, with the first factor showing a strong association among Cu, Au, and Mo, three key elements indicative of porphyry-style mineralization. This pattern suggests that magmatic and hydrothermal processes have played a critical role in the enrichment of these elements. The spatial

distribution of anomalies demonstrates a clear correlation between these elements and specific intrusive units, particularly quartz diorite to granodiorite bodies, referred to as the Shadan porphyry. These intrusions, along with silicified-carbonate breccia veins formed through tectonic and hydrothermal activity, serve as key hosts for mineral deposition. The simultaneous enrichment of Cu, Au, and Mo in these zones, along with their geochemical behavior and distribution, confirms the presence of a large porphyry system. Additionally, strong correlations between Ni–Cr and Pb–Zn were observed. Ni and Cr are likely derived from mafic–ultramafic sources, suggesting a deep-seated magmatic origin. Pb and Zn, commonly associated with the upper zones of porphyry systems, further support the presence of a zoned hydrothermal system in the area. Overall, the integration of geochemical and geological data confirms that the Shadan region hosts a significant porphyry system, making it a promising target for further mineral exploration, particularly for Au, Cu, and Mo.

Ethical Considerations

The authors avoided data fabrication, falsification, and plagiarism, and any form of misconduct.

Funding

This research did not receive any specific grant from funding agencies in the public, commercial, or not-for-profit sectors.

Conflict of Interest

The authors declare no conflict of interest.

References

[1] Granian, H., Tabatabaei, S. H., Asadi, H. H. and Carranza,. E. J. M. (2015). Multivariate regression analysis of lithogeochemical data to model subsurface mineralization: a case study from the Sari Gunay epithermal gold deposit, NW Iran. *Journal of Geochemical Exploration*, 148, 249-258. https://doi.org/10.1016/j.gexplo.2014.10.009

[2] Hezarkhani, A. (2006). Geochemistry of the Enjerd skarn and its association with copper mineralization, northwestern Iran. International Geology Review, 48(10), 892-909. https://doi.org/10.2747/0020-6814.48.10.892

[3] Keykha Hoseinpoor M. and Aryafar, A. (2014). The use of robust factor analysis of compositional geochemical data for the recognition of the target area in Khusf 1: 100000 sheet, South Khorasan, Iran. *International Journal of Mining and Geo-Engineering*, 48(2), 191-199. https://doi.org/10.22059/ijmge.2014.53107

[4] Yazdi, M., Sakhdari, M., Behzadi, M. and Mousa Zadeh, H. (2009). Geochemical exploration gold in Shanegh area, Delijan, Isfahan. *Geochimica et Cosmochimica Acta Supplement*, 73, A1482. https://doi.org/10.22059/ijmge.2014.53107

[5] Filzmoser, P. and Hron, K. (2009). Correlation analysis for compositional data. *Mathematical Geosciences*, 41, 905-919.

[6] Aitchison, J. (1982). The statistical analysis of compositional data. *Journal of the Royal Statistical Society: Series B (Methodological)*, 44(2), 139-160.

[7] Reimann, C., Filzmoser, P., Garrett, R. and Dutter, R. (2011). Statistical data analysis explained: applied environmental statistics with R. John Wiley & Sons. https://books.google.com/books?id=EyjYMb-mTfAC

[8] Filzmoser, P., Hron, K. and Reimann, C. (2009). Univariate statistical analysis of environmental (compositional) data: problems and possibilities. *Science of the Total Environment*, 407(23), 6100-6108. https://doi.org/10.1016/j.scitotenv.2009.08.008

[9] Egozcue, J. J., Pawlowsky-Glahn, V., Mateu-Figueras, G. and Barcelo-Vidal, C. (2003). Isometric logratio transformations for compositional data analysis. *Mathematical geology*, 35(3), 279-300. https://doi.org/10.1023/A:1023818214614

[10] Martín-Fernández, J. A., Barceló-Vidal, C. and Pawlowsky-Glahn, V. (2003). Dealing with zeros and missing values in compositional data sets using nonparametric imputation. *Mathematical Geology*, 35, 253-278. https://doi.org/10.1023/A:1023866030544

[11] Hron, K., Templ, M. and Filzmoser, P. (2010). Imputation of missing values for compositional data using classical and robust methods. *Computational Statistics & Data Analysis*, 54(12), 3095-3107. https://doi.org/10.1016/j.csda.2009.11.023

[12] Reimann, C., Filzmoser, P. and Garrett, R. G. (2002). Factor analysis applied to regional geochemical data: problems and possibilities. *Applied geochemistry*, 17(3), 185-206. https://doi.org/10.1016/S0883-2927(01)00066-X

[13] Martín-Fernández, J. A., Hron, K., Templ, M., Filzmoser, P. and Palarea-Albaladejo, J. (2012). Model-based replacement of rounded zeros in compositional data: classical and robust approaches. *Computational Statistics & Data Analysis*, 56(9), 2688-2704. https://doi.org/10.1016/j.csda.2012.02.012

[14] Pawlowsky-Glahn, V., Egozcue, J. J. and Tolosana-Delgado, R. (2015). Modeling and analysis of compositional data. John Wiley & Sons. https://doi.org/10.1002/9781119003144

[15] Iwamori, H., Yoshida, K., Nakamura, H., Ueki, K. et al. (2017). Classification of geochemical data based on multivariate statistical analyses: Complementary roles of cluster, principal component, and independent component analyses. *Geochemistry, Geophysics, Geosystems*, 18(3), 994-1012. https://doi.org/10.1002/2016GC006663

[16] Lin, X., Hu, Y., Meng, G., and Zhang, M. (2020). Geochemical patterns of Cu, Au, Pb and Zn in stream sediments from Tongling of East China: Compositional and geostatistical insights. *Journal of Geochemical Exploration*, 210, 106457. https://doi.org/10.1016/j.gexplo.2019.106457

[17] Hosseinpoor, M. K., Moini, H., and Torab, F. M. (2015). Detecting and mapping compositional global outliers to identify mineral exploration targets, Case study: Khusf district, East of Iran. Proc, 6th Int Conference and Workshop on Compositional Data, L'Escala, Girona, Spain. http://ima.udg.edu/codapa

[18] Torab, F. (2015). Studying the application of self organizing map (SOM) in geochemical data clustering of stream sediment and comparing the results with compositional data dendrogram. *Journal of Mining Engineering*, 10(27), 95-107. 20.1001.1.17357616.1394.10.27.9.2

[19] Keykha Hoseinpoor M. and Aryafar, A. (2016). Using robust staged R-mode factor analysis and logistic function to identify probable Cu-mineralization zones in Khusf 1: 100,000 sheets, east of Iran. *Arabian Journal of Geosciences*, 9, 1-11. https://doi.org/10.1007/s12517-015-2266-9

[20] Moini, H. and Keykha Hosseinpour, M. (2017). Fuzzy clustering analysis of compositional data and comparing it with exploratory compositional data dendrogram, case study: Anar region stream sediments geochemistry. *Journal of Analytical and Numerical Methods in Mining Engineering*, 6(12), 11-19.

[21] Buccianti A. and Pawlowsky-Glahn, V. (2005). New perspectives on water chemistry and compositional data analysis. *Mathematical Geology*, 37, 703-727. https://doi.org/10.1007/s11004-005-7376-6

[22] Carranza, E. J. M. (2011). Analysis and mapping of geochemical anomalies using logratio-transformed stream sediment data with censored values. *Journal of Geochemical Exploration*, 110(2), 167-185. https://doi.org/10.1016/j.gexplo.2011.05.007

[23] Tyler, D. E. (2008). Robust Statistics: Theory and Methods. *Journal of the American Statistical Association*, 103(482), 888–889. https://doi.org/10.1198/jasa.2008.s239

[24] Hosseini, S. A., Eftekhari Mahabadi, S. and Asghari, O. (2015). The comparison of appropriate methods in imputation of the censored values in the geochemical datasets. *Journal of Analytical and Numerical Methods in Mining Engineering*, 5(9), 63-72.

https://doi.org/10.17383/S2251-6565(15)940916-X
[25] Palarea-Albaladejo, J., Martin-Fernandez, J. A. and Palarea-Albaladejo, M. J. (2025). zCompositions-R package
[26] Johnson, R. A. and Wichern, D. W. (2002). *Applied multivariate statistical analysis*.
[27] Taylor S. R., and McLennan, S. M. (1985). The continental crust: its composition and evolution.
[28] Sillitoe, R. H. (2010). Porphyry copper systems. *Economic geology*, 105(1), 3-41. https://doi.org/10.2113/gsecongeo.105.1.3
[29] Seedorff, E., Dilles, J. H., Proffett, Jr., J. M., Einaudi, M. T., Zurcher, L., Stavast, W. J. A., Johnson, D. A., Barton, M, D. (2005). Porphyry Deposits: Characteristics and Origin of Hypogene Features. In: Hedenquist, J. W., Thompson, J. F. H., Goldfarb, R. J., Richards, J. P. (Eds) One Hundredth Anniversary Volume, Society of Economic Geologists. https://doi.org/10.5382/AV100
[30] Richards, J. (2003). Tectono-magmatic precursors for porphyry Cu-(Mo-Au) deposit formation. *Economic geology*, 98(8), 1515-1533. https://doi.org/10.2113/gsecongeo.98.8.1515